CORE
Metadata, citation and similar papers at core.ac.uk
Provided by Elsevier - Publisher Connector

Virology 437 (2013) 89–99

Contents lists available at SciVerse ScienceDirect

Virology

journal homepage: www.elsevier.com/locate/yviro

Virions proteins of an RSIV-type megalocytivirus from spotted knifejaw *Oplegnathus punctatus* (SKIV-ZJ07)

Fan Shuang [a], Yongwen Luo [a], Xiao-peng Xiong [a], Shaoping Weng [a], Yiming Li [a], Jianguo He [a,b,*], Chuanfu Dong [a,**]

[a] MOE Key Laboratory of Aquatic Food Safety/State Key Laboratory for Bio-control, School of Life Sciences, Sun Yat-sen University, Guangzhou 510275, People's Republic of China
[b] School of Marine Sciences, Sun Yat-sen University, Guangzhou 510275, People's Republic of China

ARTICLE INFO

Article history:
Received 11 September 2012
Returned to author for revisions
24 October 2012
Accepted 29 December 2012
Available online 24 January 2013

Keywords:
Iridovirus
Megalocytivirus
Proteomics
Virus induced stress protein (VISP)
Envelope protein

ABSTRACT

Megalocytiviruses have three main genotypes, which are represented by ISKNV, RSIV, and TRBIV. To date, the virion-associated proteins of RSIV and TRBIV are still unknown. The spotted knifejaw iridovirus (SKIV) is a newly characterized RSIV-type megalocytivirus. In this study, the virion-associated proteins of SKIV were identified by systemic one-dimensional gel electrophoresis-based proteomic approaches. A total of 49 viral proteins and 33 cellular proteins were associated with the SKIV virions by LC MS/MS, including 18 highly abundant structural proteins that were detected by MALDI TOF/TOF-MS. One highly abundant structural protein of interest was identified as the virus-inducible stress protein (VISP) and further characterized as an envelope protein. However, knockdown of mVISP by siRNA method showed no effect in virion production. The current study is the first to present detailed information on the virion-associated proteins of an RSIV-type megalocytivirus and to identify a novel cellular envelope protein of this virus.

© 2013 Elsevier Inc. All rights reserved.

Introduction

The Iridoviridae family is composed of icosahedral large cytoplasmic dsDNA viruses that are classified into five genera: *Iridovirus*, *Chloriridovirus*, *Ranavirus*, *Lymphocystivirus*, and *Megalocytivirus,* according to the Ninth Report of the International Committee on Taxonomy of Viruses (Jancovich et al., 2012). Among these viruses, the lymphocystiviruses, ranaviruses, and megalocytiviruses have been confirmed as the important causative agents of serial, high-mortality diseases in finfish. Thus, these viruses are collectively known as the piscine iridoviruses, with the megalocytiviruses being the latest genus to be identified (Chinchar et al., 2005). The red sea bream iridovirus (RSIV) was the first megalocytivirus to be reported (Inouye et al., 1992), which has been associated with mass mortalities of over 30 cultured marine fish species in Japan since its first occurrence in the late 1980s (Kawakami and Nakajima, 2002). In China, megalocytivirus-induced mass mortalities were first documented in freshwater cultured mandarin fish in the early 1990s (He et al., 2000), which were attributed to the infectious spleen and kidney necrosis virus (ISKNV) based on its clinical signs and histopathological profiles (He et al., 2001). Molecular epidemiology investigations have indicated that the ISKNV-like megalocytiviruses can infect over 50 cultured and wild marine fish species in the South China Sea (Wang et al., 2007). Apart from RSIV and ISKNV, other megalocytiviruses include the turbot reddish body iridovirus (TRBIV) (Shi et al., 2010) and orange spotted grouper iridovirus (OSGIV) (Lü et al., 2005; Ma et al., 2012) in China, the rock sea bream iridovirus (RBIV) in South Korea (Do et al., 2004), and the Murray cod iridovirus in Australia (Go et al., 2006), as well as several other fish iridovirus species in Southeast Asian countries and regions (Jancovich et al., 2012; Kurita and Nakajima, 2012). Most recently, natural outbreaks of megalocytivirus-associated diseases were first recorded in North America in a wild, temperate, indigenous fish species, the three-spined stickleback (*Gasterosteus aculeatus*) (Marcos-López et al., 2011; Waltzek et al., 2012). Thus, megalocytiviruses have attracted much attention since the late 1980s because of their capacity to cause serious systemic diseases in a wide-range of economically important freshwater and marine fish species in the Asia-Pacific region (Kurita and Nakajima, 2012; Subramaniam et al., 2012). RSIV and ISKNV have been extensively studied, and ISKNV was defined as the type species of the genus *Megalocytivirus* (Chinchar et al., 2005; Jancovich et al., 2012).

A phylogenetic analysis that was based on the major capsid protein (MCP) gene, which is a conserved core viral gene in

* Corresponding author at: School of Life Sciences, Sun Yat-sen University, No. 135, Xingang Road West, Guangzhou 510275, People's Republic of China. Fax: +86 2084113229.
** Correspondence to: School of Life Sciences, Sun Yat-sen University, No. 135, Xingang Road West, Guangzhou 510275, People's Republic of China. Fax: +86 20 84113229.
E-mail addresses: lsshjg@mail.sysu.edu.cn (J. He), dongchuanfu999@163.com, dongchfu@mail.sysu.edu.cn (C. Dong).

0042-6822/$ - see front matter © 2013 Elsevier Inc. All rights reserved.
http://dx.doi.org/10.1016/j.virol.2012.12.017

iridoviruses, showed that most megalocytiviruses can be divided into three main groups, namely, the ISKNV, RSIV, and TRBIV types (Kurita and Nakajima, 2012). The ISKNV type includes almost all freshwater-borne megalocytiviruses. The RSIV type includes the megalocytiviruses that infect most marine fish from the order Perciformes. The TRBIV type particularly infects flatfish species such as turbot and flounder. Compared to the restricted host fish species of the ISKNV and TRBIV types, RSIV-type megalocytiviruses can infect a broader range of fish species (Dong et al., 2010; Kurita and Nakajima, 2012; Kwon et al., 2011).

A functional study of megalocytivirus proteins would be of great benefit for the prevention and control of associated diseases. The first step of functional gene analysis is to identify the structural proteins, and the structural proteins of ISKNV were comprehensively analyzed and characterized in our recent report (Dong et al., 2011). However, virion proteins of other members of megalocytiviruses remain unknown. ISKNV has always been associated with the mass mortalities of freshwater fish, but RSIV can infect a broader range of marine fish species. The marine fish have always been refractory to ISKNV infection in artificial condition (He et al., 2002); however, the RSIV from marine fish is highly pathogenic to freshwater mandarin fish, the most-susceptible hosts of ISKNV infection, both in artificial and natural conditions (Dong et al., 2010; Fu et al., 2011). Other differences were observed in the virion array of ISKNV and RSIV. Since the first reported occurrence of ISKNV in China in the early 1990s, an irregular random array of viral particles has always been observed in infected fish tissues and mandarin fish fry (MFF-1) cells using transmission electron microscopy (TEM). By contrast, large amounts of RSIV virions in a regular paracrystalline array were observed in both RSIV-infected MFF-1 cells and mandarin fish tissues (Dong et al., 2010). The factors that cause these differences among these types of megalocytiviruses are still unknown. Therefore, an exploration of the virion-associated proteins from different types of viruses may help to understand these differences. A few studies have attempted to determine the structural proteins of RSIV (Nakajima et al., 1998); however, these have generally been limited in scope.

The spotted knifejaw iridovirus (SKIV) is a highly virulent megalocytivirus that was isolated and characterized from a mass mortality of spotted knifejaw (*Oplegnathus punctatus*) (Dong et al., 2010). According to phylogenetic analysis, SKIV belongs to the RSIV genotype of megalocytiviruses. This cluster includes other well-known marine fish megalocytiviruses such as OSGIV from China, a series of RSIV strains from Japan, some RBIV strains from South Korea, and several strains of grouper iridoviruses from Singapore and other countries and regions (Dong et al., 2010). In this study, we purified the SKIV virion particles and identified the viral proteins using a proteomic approach. Aside from a traditional one-dimensional gel electrophoresis (1-DE) workflow to separate the viral proteome (1-DE-MALDI workflow), we established a liquid chromatography (LC)-matrix-assisted laser desorption/ionization (MALDI) tandem mass spectrometry (MS/MS) analysis workflow (LC-MALDI workflow). The combined workflows greatly expanded the number of proteins that were identified in the SKIV-ZJ07 proteome. A virus-inducible stress protein of interest, which was highly abundant in the purified SKIV particles, was designated as mVISP and identified as a novel cellular envelope protein of SKIV virions. The functional profiles of mVISP in infection in MFF-1 cells were likewise investigated.

Results

Major structural proteins by 1-DE-MALDI workflow

SKIV-ZJ07 was purified using sucrose gradient ultracentrifugation. Numerous spherical virions with intact membrane structures were observed using TEM (Fig. 1B). SDS-PAGE analysis showed that SKIV-ZJ07 contained 19 visible protein bands (Fig. 1C). Subsequently, all the bands were excised from the gel for further MS analysis. Following trypsin digestion of the reduced and alkylated protein bands, the resulting peptides were analyzed by MALDI-TOF/TOF-MS. The MS data for each digested protein were used to query the NCBInr database using the MASCOT Version 2.2 (Matrix Science, London, UK) search engine to identify the proteins and corresponding genes. Among the obtained 20 peptide mass fingerprinting (PMF) maps that were combined with the MS/MS data, 19 PMFs matched to 18 megalocytiviral proteins (Table 1). All the 18 identified viral proteins first matched to the RSIV-type megalocytiviruses like OSGIV, RBIV, and RSIV and second matched to ISKNV and TRBIV. Thus, using OSGIV (Lü et al., 2005) as the reference template, these proteins were designated as the OSGIV-ORF062L, -ORF075L, -ORF063L, -ORF071L, -ORF087R, -ORF040L, -ORF113R, -ORF039L, -ORF008L, -ORF007L (MCP), -ORF055L, -ORF0038L, -ORF007L (repeat identification of MCP), -ORF112L, -ORF056L, -ORF121L, -ORF097L, -ORF080R, and -ORF019R. The profiles of the identified proteins were highly consistent with our previous results in ISKNV virions (Dong et al., 2011). For instance, band 6 was identified as a mixture of OSGIV-ORF087 and RBIV-ORF038 proteins, which corresponds to a mixture of the ISKNV-ORF088R and -ORF038L protein in band 6 of the ISKNV virions (Dong et al., 2011). In ISKNV virions, the MCP, ISKNV-ORF055L, -ORF125L, and -ORF101L were the most abundant viral proteins. Their corresponding proteins in SKIV were similarly the most abundant. However, some differences were observed. For example, a putative phosphatase (corresponding to ISKNV-ORF022L) was identified as a major viral protein in our previous work (Dong et al., 2011), but this protein was not identified by the 1-DE-based proteomic approach in the current work. By contrast, ISKNV-ORF115 was not a highly abundance viral protein in our previous work, but its homolog in SKIV (OSGIV-ORF112L) was identified in this work. RSIV-321R,

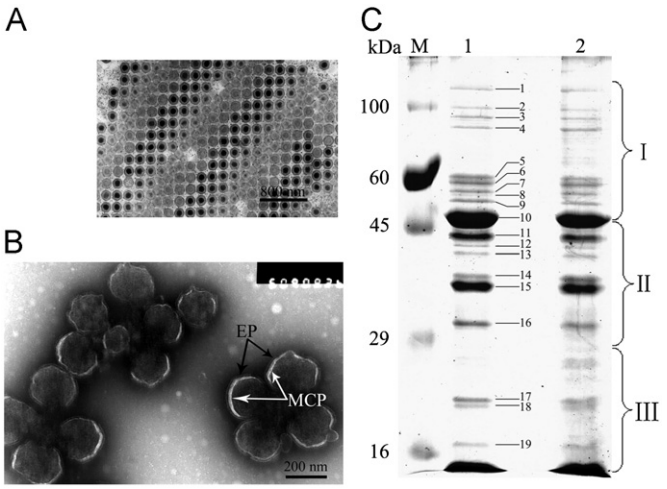

Fig. 1. Major structural protein profiles of purified SKIV-ZJ07 virions. (A) TEM micrograph of SKIV-ZJ07 infected MFF-1 cells. Numerous paracrystalline array mature viruses were observed in cytoplasm in infected MFF-1 cells, bar=800 nm. (B) TEM observation of purified SKIV-ZJ07 virions. The black arrows indicate the thin envelope protein (EP) layer in purified virions; the white arrows indicate the thick MCP layer located inside EP layer, bar=200 nm. (C) Viral proteins from the purified virus were separated by 12% gradient SDS-PAGE gels and visualized by Coomassie brilliant blue R-250 staining. Proteins in lane 1 were used for MALDI-TOF/TOF-MS analysis. Numbers indicate the excised protein bands. The lane 2 gel was cut into three equal pieces according to molecular mass weight. The gel pieces are designated as fractions I, II, and III, and then were performed for LC–MS/MS analysis, respectively. M, broad range pre-stained protein marker (NEB).

Table 1
Identification of the major structural proteins of SKIV-ZJ07 by MALDI-TOF MS/MS.

Band	Accession nos.	Best match to megalocytiviral protein/ORF	Matched peptides numbers	MW/PI	Protein score	Predicted structure and/or function[a]	Homology to megalocytiviral ORF			
							RBIV	OSGIV	ISKNV[b]	TRBIV
1	gi|50237540	RBIV-DBP	28	143903.5/5.53	349	DBP	058L	062L	062L	057L
2	gi|62421264	OSGIV-ORF075L	26	111945.3/6.33	278	TM	072L	075L	076l	069R
3	gi|50237541	RBIV-ORF059L	19	100805.6/9.2	209	TM; Putative NTPase;	059L	063L	063L	058L
4	gi|24637709	–	19	79790.8/4.47	192	VISP	–	–	–	–
5	gi|50237550	RBIV-ORF068L	6	53226.9/6.3	86	TM	068L	071L	071L	065L
6	gi|62421276	OSGIV-ORF087R	18	58528.6/8.9	132	TM	084R	087R	088R	081R
6	gi|50237520	RBIV-ORF038L	12	56577.8/7.33	101	TM	038L	040L	038L	037L
7	gi|62421310	OSGIV-ORF113R	5	41554.4/4.99	86	TM	111R	113R	117R	108R
8	gi|113200504	LYCIV-ORF037L	12	49902/6.14	118	TM	037L	039L	037L	036L
9	gi|62421197	RBIV-ORF008L	11	51502.5/8.63	103	MMP; TM	08L	008L	007L	07L
10	gi|109452566	RSIV-MCP	9	48263.1/6.01	289	MCP; TM	007L	007L	006L	006L
11	gi|62421244	OSGIV-ORF055L	11	35245.6/5.63	240	Virus-specific 2-cysteine adapter	052L	055L	054L	051L
12	gi|62421227	OSGIV-ORF038R	12	38392.5/	67	No hit	–	038R	036R	035R
13	gi|109452566	RISV-MCP	6	48263.1/6.01	108	MCP,TM	007L	007L	006L	006L
14	gi|62421301	OSGIV-ORF112L,	10	38167/6.78	92	ICP46	108L	112L	115L	106L
15	gi|50237535	RBIV-ORF053L,	21	34437/10.24	359	S/TPK; RGD	053L	056L	055L	052L
16	gi|62421309	OSGIV- ARP	9	25004.5/6.1	141	ARP; TM; RGD	118L	121L	125L	115L
17	gi|62421286	OSGIV-ORF097L	8	19100.4/5.56	224	No hit	–	097L	101L	092L
18	gi|62421269	OSGIV-080R	6	18569.6/6.05	110	No hit	078R	080R	081R	074R
19	gi|327396900	RSIV-321R	3	12480/7.90	113	TM	017R	019R	–	017R

DBP, DNA binding protein; TM, trans-membrane domain; VISP, virus-inducible stress protein [*Oncorhynchus tshawytscha*]; RGD, Arg–Gly–Asp domain; MMP, myristylated membrane protein; MCP, major capsid protein; S/TPK, serine–threonine protein kinase; ARP, ankyrin repeat protein; ISKNV, infectious spleen and kidney necrosis iridovirus; RBIV, rock bream iridovirus; OSGIV, orange spotted grouper iridovirus; TRBIV, turbot reddish body iridovirus; RSIV, red seabream iridovirus; LYCIV, large yellow croacker iridovirus.

[a] Structure and/or function were predicted with Smart Server (http://smart.embl-heidelberg.de/smart/change_mode.pl) combined with TMpred Server (http://www.ch.embnet.org/software/TMPRED_form.html) according to operation instruction.

[b] ISKNV ORFs were obtained from the mirror site of National Center for Biotechnology Information (NCBI) nucleotide database using blastp tool.

a low-mass/weight protein corresponding to OSGIV-ORF019L, was likewise identified as a major viral protein in SKIV virions.

No reliable matches to a highly abundant protein in band 4 (Fig. 1B, band 4) were found even when its PMF was acquired. Further MALDI-TOF-MS/MS analysis revealed that the 19 acquired peptides from band 4 matched a cellular, virus-inducible stress protein *Ot*VISP (Fig. S1). Given that this cellular protein was derived from SKIV-infected MFF-1 cells, the protein was designated as the virus-inducible stress protein from mandarin fish cells, mVISP.

Virion-associated proteins by LC–MS/MS workflow

The tryptic peptide mixture of the SKIV-ZJ07 proteins was separated using a reverse phase nano-LC column after the three gel-separated virion fractions were digested by trypsin. For each fraction, three separate LC–MALDI runs were performed with various acetonitrile gradients to ensure the effective separation of peptides with different levels of hydrophobicity. All the MS/MS spectra from the three runs were combined for the database search to maximize the sensitivity and reliability of protein identification. Only peptides with a 95% confidence level or higher were considered. Thus, a total of 49 proteins were identified, each with at least one peptide that matched to the megalocytiviral proteins (Table 2). More detailed information on the MS data for these viral proteins was provided in the Supplementary Document 2 (Table S2). The amino acid coverage of the individual identified proteins ranged from 8.26% to 82.02%. The identified proteins contained at least one top-ranked peptide with a MASCOT expectation value of < 0.05. From the matching priority, 42 proteins were first matched to proteins from OSGIV (23 unique proteins), RBIV (3 unique proteins) or both (16 proteins). However, only 5 proteins (including 4 unique proteins) were first matched to proteins from ISKNV. The results indicated that SKIV-ZJ07 would be more similar to the OSGIV and RBIV strains than to the ISKNV and TRBIV strains. As expected, all 18 major viral proteins that were previously identified by MALDI-TOF-MS/MS were similarly found in these 49 proteins. The analysis showed that 40 proteins had a variety of functional domains, which included 20 transmembrane domains, 3 ankyrin repeat protein (ARP) domains, 3 Arg–Gly–Asp (RGD) domains, and 2 serine/threonine protein kinase (S/T-PK) domains, among others. The identified proteins were derived from sucrose gradient ultracentrifugation. Thus, the frequency of non-structural proteins was relatively very low, and most of the LC–MS/MS-identified proteins were suspected to be structural proteins of SKIV-ZJ07.

Apart from the 49 viral proteins, 33 additional cellular proteins were identified by LC–MALDI MS/MS. These proteins included 5 chaperones or chaperone-like proteins, 3 cytoskeletal proteins, 14 ribosomal proteins, 4 metabolism-associated proteins, and 7 other functional proteins (Table 3). The detailed MS data information for these cellular proteins was presented in Supplementary Document 3 (Table S3). With the exception of two proteins from *Xenopus laevis* (African clawed frog), all the cellular proteins were from teleost species. As expected, *Ot*VISP was also included in this list (Table 3).

Cloning, expression, and antigenicity of partial fragments of mVISP

According to the nucleotide sequences that correspond to the acquired matched peptides in *Ot*VISP (Fig. S1), two pairs of primer sets were designed to clone and express the corresponding mVISP fragment using the cDNA from SKIV-infected MFF-1 cells as the template. Sequence alignment analysis showed that the cloned nucleotides sequence from the MFF-1 cells were 99% identical to that of *Ot*VISP (data not shown). Protein expression and purification were then conducted using the pMAL-c2x expression and purification system. Two recombinant proteins were obtained,

Table 2
Virions-associated viral proteins of SKIV-ZJ07 identified by 1-DE-gel based RP-LC MS/MS.

No.	% Cov (95)	Protein ID	Matched peptides number	Predicted structure and/or function	Homology to megalocytiviral ORF			
					RBIV	OSGIV	ISKNV	TRBIV
1	43.18	Q5YF29	37	Putative DNA-binding protein	*058L*	062L	062L	057L
2	48.99	Q4KS82	29	No hit	072L	*075L*	076L	069R
3	30.95	Q4KS94	25	SNF2 family helicase	059L	*063L*	063L	058L
4	63.58	Q5YF34, 4KSA1	22	S/T-PK; RGD	*053L*	*056L*	055L	052L
5	56.07	Q6QNG5, 4KSF0	22	Major capsid protein; TM	*007L*	*007L*	006L	006L
6	82.02	Q4KS36	19	ARP; RGD	–	*118L*	125L	115L
7	49.72	Q71G61	18	*RSIV Putative phosphatase*	022L	025L	022L	023L
8	54.64	Q5YF79, 4KSE9	18	MMP; TM	*008L*	*008L*	007L	007L
9	68.15	Q4KSA2	15	Virus-specific 2-cysteine adapter	052L	*055L*	054L	051L
10	33.59	Q4KS86	12	TM	068L	*071L*	071L	065L
11	34.8	Q4KS70	11	TM	084R	*087R*	088R	081R
12	44.19	Q5YEZ9,Q4KS65	10	No hit	*088L*	*092L*	095L	087L
13	27.7	Q4KS81	8	ARP	–	*076R*	077R	070R
14	19.83	Q4KSB7	6	TM	038L	*040L*	038L	037L
15	33.63	Q5YF45, Q4KSB4	7	TM	*042L*	*043L*	041L	040L
16	8.26	Q4KS51	5	D5 family NTPase; TM	101L	*106L*	109L	099L
17	26.19	Q4KS45	6	ICP-46	108L	*112R*	115R	106R
18	34.09	Q5YF01, Q4KS67	6	No hit	*086L*	*090L*	093L	085L
19	25.31	Q5YF73, Q4KSE1	5	TM	*014R*	*016R*	014R	014R
20	20.04	Q5YF29	6	*LYCIV-ORF037L, RGD; TM*	037L	039L	037L	036L
21	58.48	Q8QUK9	5	No hit	102L	097L	*101L*	092L
22	19.45	Q4KS42	5	ARP	112L	*115L*	119L	109L
23	40.93	Q8QUQ4	5	No hit	054L	057L	*056L*	053L
24	14.05	Q5YF23, Q4KS88	5	TM	*064L*	*069L*	068L	063L
25	56.36	Q4KS77	5	No hit	078R	*080R*	081R	074R
26	51.67	Q4KSB2	4	Thiol oxidoreductase; TM	–	*045L*	043L	042L
27	26.21	Q4KSB9	5	TM	–	*038R*	036R	035R
28	8.47	Q4KS46	5	Tyrosine kinase; TM	106L	*111L*	114L	105L
29	23.7	Q4KS44	4	TM	110R	*113R*	117R	106R
30	33.12	Q5YF12, Q4KS80	4	No hit	*075R*	*077R*	078R	071R
31	17.82	Q5YF02	4	TM	*085L*	–	–	083L
32	19.13	Q5YF59, Q4KSC7	4	DNA repair protein RAD2; TM	*028L*	*030L*	027L	027L
33	23.7	Q4KS43	4	Early 31 kDa-protein	111L	*114L*	118L	108L
34	20.55	Q4KSB6	4	TM	–	*041R*	039R	038R
35	15.9	Q4KS38, Q77HV8	3	ATPase	119R	*116R*	*122R*	113R
36	17.91	Q4KS97	3	Putative replication factor; TM	057L	*060L*	057L	056L
37	33.53	Q5YF31, Q4KS98	3	TM;	*056L*	*059L*	–	055L
38	9.16	Q8QUV4	2	CTD-like phosphatase	006L	006L	*005L*	005L
39	14.88	Q5YEZ5, Q4KS61	2	No hit	*092L*	*096L*	100L	091L
40	8.9	Q5YF46, Q4KSB5	2	TM	*041L*	*042L*	040L	039L
41	9.89	Q8QUU5	2	S/T-PK	015R	013R	*015R*	015R
42	38.46	Q5YF76	2	TM	*011L*	011L	010L	010L
43	15.15	Q5YF07, Q4KS75	2	No hit	*080R*	*082R*	–	076R
44	11.41	Q50JU0	2	*RSIV TRAF-2 like protein; TM*	102L	108L	111L	101L
45	18.25	Q4KS58	2	SOCS-like protein	–	*099R*	103R	094R
46	13.4	Q4KS48	2	Proliferating cell nuclear antigen	103R	*109R*	112R	102R
47	16.96	Q5YF70, Q4KSD8	1	TM	*017R*	*019R*	–	017R
48	6.02	Q5YF43	1	No hit	*044L*	046L	044L	
49	9.67	Q5YF26, Q4KS92	1	RING-finger; E3 ubiquitin ligase; TM	*061L*	*065L*	065L	060L

The italics indicate the best matched proteins/ORFs (the protein ID represented protein). If the italics covers both two areas, it means the acquired MS data are matched to both virus species. Detailed MS data can be found in Table S2.

both mainly water-soluble (Fig. 3A). The soluble recombinant proteins were further purified (Fig. 3B). WB analysis showed that the recombinant proteins could be effectively recognized by the rabbit anti-ISKNV anti-serum (Fig. 3C).

Localization of mVISP in SKIV virions by SDS-PAGE and WB analysis

The anti-serum was prepared using purified pMAL-mVISP-F2 as the antigen to immunize the rabbits. The purified virions were divided into two fractions by treatment with 1% Triton X-100 to localize the mVISP protein in SKIV virions. SDS-PAGE showed that mVISP mainly existed in the supernatant fraction of the Triton-X-treated SKIV solution, whereas the DNA-binding protein, a known viral component within the virion core, was found to exist solely in the pellet fraction (Fig. 4A). MCP was similarly found in the pellet fraction (Fig. 4A). These results were further confirmed by WB analysis using rabbit anti-ISKNV serum as the primary antibody (Fig. 4B). The fractionated viral components were further validated by WB analysis using the anti-ISKNV-MCP, anti-ISKNV-MMP, and anti-mVISP anti-sera as the primary antibodies. As panel controls, MCP and MMP were mainly found to exist in the pellet and supernatant fractions, respectively, of the fractionated SKIVs (Fig. 4C and D). These results were highly consistent with their locations in ISKNV virions in our previous report (Dong et al., 2011). Consistent with the well-known envelope protein ISKNV-MMP, mVISP was similarly found to exist mainly in the supernatant fraction of the fractionated SKIVs (Fig. 4E).

Visual localization of mVISP via IEM

IEM showed that gold particles were specifically located on the envelopes of the virions when the anti-mVISP serum was used

Table 3
Virions-associated cellular proteins of purified SKIV-ZJ07 identified by 1-DE-gel based RP-LC MS/MS.

No.	Proteins description	Species[a]	Sequence cov (%)	Protein ID	Peptide number	Predicted function
1	Virus-inducible stress protein	*Oncorhynchus tschawytscha*	42.74	Q8AYC5	19	Chaperone-like proteins
2	MGC53952 protein	*Xenopus laevis*	14.40	Q7ZTK6	7	Chaperone (HSP70 family)
3	Glucose-regulated protein 78	*Paralichthys olivaceus*	7.33	A5H1H9	3	Chaperone (HSP70 family)
4	HSP90 - (European sea bass)	*Dicentrarchus labrax*	6.62	Q6TL18	3	Chaperone
5	HSP60 - (Goldfish)	*Carassius auratus*	12.35	Q0GC54	3	Chaperone
6	Beta-tubulin	*Notothenia coriiceps*	39.33	Q9DFT6	13	Cytosteleton
7	Alpha-tubulin	*Danio rerio*	28.28	Q6NWK7	7	Cytosteleton
8	Beta-actin	*Dicentrarchus labrax*	23.73	Q6YI33	7	Cytosteleton
9	Ribosomal protein L4	*Pagrus major*	26.98	Q6Y213	8	Translation
10	Ribosomal protein S13	*Danio rerio*	28.48	Q6IMW6	6	Translation
11	Ribosomal protein S2	*Solea senegalensis*	21.79	A2Q0R6	4	Translation
12	60S ribosomal protein L27	*Fundulus heteroclitus*	41.32	Q5XVN9	5	Translation
13	Ribosomal protein S6	*Solea senegalensis*	14.46	A2Q0S1	4	Translation
14	40S ribosomal protein S7	*Perca flavescens*	33.51	A7UIU8	4	Translation
15	60S ribosomal protein L17	*Scophthalmus maximus*	21.18	A0EZV0	3	Translation
16	40S ribosomal protein S15A	*Paralichthys olivaceus*	40.77	Q9IA74	3	Translation
17	Ribosomal protein S9	*Danio rerio*	10.82	Q6P5M3	2	Translation
18	Ribosomal protein S3	*Danio rerio*	14.69	Q6TLG8	2	Translation
19	40s ribosomal protein S27a	*Epinephelus coioides*	28.21	Q8JJ02	3	Translation
20	Ribosomal protein L30	*Danio rerio*	23.93	Q7ZUG6	3	Translation
21	40S ribosomal protein S17	*Siniperca chuatsi*	38.06	Q2KKZ3	3	Translation
22	Ribosomal protein S16	*Solea senegalensis*	13.04	A2Q0T2	2	Translation
23	GAPDH	*Danio rerio*	15.82	Q6NYM9	4	Metabolism
24	V-type ATPase B subunit	*Oncorhynchus mykiss*	10.96	Q9W6M4	4	Metabolism
25	Putative RNA helicase	*Danio rerio*	6.25	O42375	3	Metabolism
26	ATPase, H+ transporting, lysosomal 70 kDa, V1 subunit A, like	*Danio rerio*	7.13	Q7SY46	3	Metabolism
27	Voltage-dependent anion channel	*Paralichthys olivaceus*	29.33	A1Y189	5	Apoptosis
28	Chromosome 6 SCAF14544	*Tetraodon nigroviridis*	20.00	Q4SMV9	5	Insulin receptor binding
29	MGC80936 protein	*Xenopus laevis*	4.30	Q6GNR4	4	Clathrin coat of coated pit
30	Programmed cell death 6	*Danio rerio*	28.11	Q7T3D5	3	Apoptosis
31	Chromosome 7 SCAF15001	*Tetraodon nigroviridis*	18.73	Q4RS35	3	Uncharacterized protein
32	Valosin containing protein	*Danio rerio*	4.71	Q7ZU99	3	Regulation
33	Annexin A5—(Nile tilapia)	*Oreochromis niloticus*	7.57	A7YIG9	2	Signaling

[a] Except for *Xenopus laevi* (African clawed frog), all other species are teleost. Detailed MS data can be found in Table S3.

as the primary antibody in the staining procedure (Fig. 5B). However, no gold particles were observed in Triton-X-100 treated non-envelope virion (Fig. 5A). In another control group, only a few gold particles were observed for SKIV virions when the pre-immune serum was used as the primary antibody (Fig. 5C).

Time course of mVISP protein expression in infected MFF-1 cells

The specific mVISP protein expression in the SKIV-infected and mock-infected MFF-1 cells at different post-infection time intervals (0, 6, 12, 24, 48, 72 and 96 hpi) were determined by WB analysis. MCP, the most abundant structural protein in SKIV, was selected as a control marker for the comparative analysis of the mVISP proteins expression. The results showed that the MCP highly expressed at 48 hpi and no detection signals were observed before at 24 hpi (Fig. 6A). By contrast, the mVISP maintained low expression at 0, 6, 12, and 24 hpi. High expression of mVISP was detected at 48 hpi up to 96 hpi, in this period, which was highly consistent with the MCP expression (Fig. 6A).

Knockdown effect of mVISP

mVISP target siRNAs were designed to block the mVISP expression in MFF-1 cells. The results showed that the siRNAs could effectively down-regulate the mVISP expression in transiently transfected MFF-1 cells. Compared with increasing expression of mVISP at 24 h post transfection in non-silencing control (Fig. 6C) and normal MFF-1 cells (Fig. 6A), the mVISP expression in siRNA group maintained stably low expression (Fig. 6B). However, MCP expression maintained similar pattern both in siRNA and NC groups (Fig. 6B and C). In iridovirus, MCP is the most important marker protein to monitor the viral replication, assemble and mature (Whitley et al., 2010). Normal expression of MCP in mVISP-blocked MFF-1 cell indicated that mVISP was not an essential factor for SKIV virion production. Moreover, $TCID_{50}$ determination confirmed that virus suspensions from siRNA and NC group yielded viral titers of $10^{6.83}$/0.1 ml and $10^{6.77}$/0.1 m at 6 dpi, respectively.

Discussion

In the first decade of the 21st century, megalocytiviruses have proven to be among the most important disease-causing agents in the finfish aquaculture industry (Kurita and Nakajima, 2012; Subramaniam et al., 2012). These viruses have been of increasing concern because of their extremely damaging effects on cultured fish. Once megalocytivirus outbreaks occur, over 50% mortality has been observed within a very short time period (Kurita and Nakajima, 2012; Ma et al., 2012). Advancements have been made toward understanding the histopathology, epidemiology, genomics, infection model, cultured cell-based vaccines and some functional genes of megalocytiviruses (Dong et al., 2012; Kurita and Nakajima, 2012; Wang et al., 2008; Xu et al., 2008, 2010a, 2010b); however, studies on the identification of virion-associated proteins generally remain limited (Dong et al., 2011). In this study, we report the identification of 49 viral proteins in

the SKIV-ZJ07 virions using a combination of 1-DE-MALDI and LC-MALDI proteomic approaches. Among these proteins, 18 were identified as highly abundant viral proteins by 1-DE gel-based approaches, whereas 31 additional viral proteins were identified by the LC-MALDI workflow (Table 2). Among the viral proteins that were identified by LC-based proteomics, some may be present in the virions in very low levels. These low-abundance proteins cannot be identified in gel-based MALDI-TOF/TOF-MS analysis because only the visible and bright bands were excised from the gels for further analysis (Song et al., 2004). Therefore, LC-based approaches have the advantage of identifying the low-abundance proteins. By contrast, the identification results by MALDI-TOF/TOF-MS are more definite and intuitive. Overall, the two workflows were complementary as well as equally effective. Both identification methods were employed to analyze the viral proteins of SKIV-ZJ07 and to characterize the highly abundant viral protein bands in the gel. Likewise, the results indicated that most of the identified proteins were first matched to OSGIV and RBIV, then to ISKNV and TRBIV, which strongly suggested that SKIV-ZJ07 was more similar to the RSIV-type than to the ISKNV- or TRBIV-type megalocytiviruses at the level of the viral proteome. Since the complete genome sequence of SKIV-ZJ07 remains unknown, the identified viral proteins from SKIV-ZJ07 have to refer to other megalocytiviral strains like OSGIV (Lü et al., 2005), RBIV (Do et al., 2004) and ISKNV (He et al., 2001), which may cause some confusion to understand SKIV proteins.

The structural proteins of an ISKNV-type megalocytivirus have been comprehensively determined and characterized, which was previously the only comprehensively characterized viral proteome in megalocytivirus (Dong et al., 2011). In the study of ISKNV proteomics, a total of 38 ISKNV-associated viral proteins were identified; 32 of these were further confirmed as structural proteins by WB analysis, which included 16 highly abundant viral proteins (Dong et al., 2011). In contrast, 49 virion-associated viral proteins, including the 18 highly abundant viral proteins of SKIV-ZJ07, were identified in the present study. The remaining homologous viral proteins in ISKNV are ISKNV-ORF114L, -ORF027L, -ORF122L, -ORF057L, -ORF005L, -ORF015R, -ORF010L, -ORF103R, -ORF112R, and -ORF065L (Fig. 2). Moreover, since no corresponding homologous proteins existed in ISKNV, four viral proteins are identified in SKIV virions using RBIV as reference. These proteins are RBIV-ORF085L, -ORF056L, -ORF080R, and -ORF017R (Fig. 2). The ISKNV-ORF012R, -ORF033L, and -ORF045L were identified in the ISKNV proteomic analysis, but their corresponding homologous proteins in the SKIV virions were not found. Overall, the number of identified viral proteins in SKIV was greater than that in ISKNV. For the remaining proteins in ISKNV, ISKNV-ORF114L and -ORF005L were found to be homologous to the in the virions of the Chilo iridescent virus, an invertebrate iridovirus in the Iridoviridae family (Ince et al., 2010). The ISKNV-ORF015R was characterized as a low-abundance viral protein in ISKNV (Xu et al., 2011). Several possible reasons may explain why these proteins were undetected in ISKNV. First, ISKNV is a distinct megalocytivirus. Thus, some non-ISKNV first-matched proteins may have been unintentionally disregarded in the previous study (Dong et al., 2011). These proteins include the RBIV-ORF085L, -ORF056L, -ORF080R, and -ORF017R. Second, most of the missing identified proteins in virions are low-abundance or low-mass/weight, which may have resulted in very low detectable levels. In addition, the differential expression of the viral proteins between ISKNV and RSIV cannot be ruled out, which may cause phenotypic variations in the virion array, host range, pathogenicity, and antigenicity of these viruses. Some non-structural proteins may be identified by a shotgun-based proteomic approach (Song et al., 2006). Most probably, not all the viral proteins that were identified in this work are viral structural proteins.

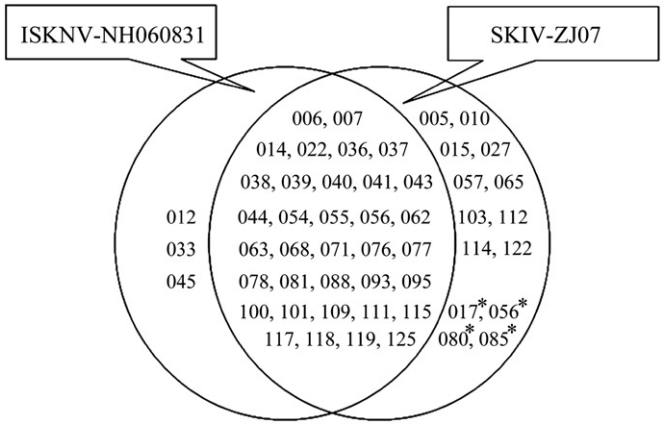

Fig. 2. A summary of virion-associated viral proteins from ISKNV-NH060831 and SKIV-ZJ07. The overlapped region represents proteins identified both in ISKNV and SKIV. The numbers in the rings regions indicate megalocytiviral ORFs numbers. Asterisks indicated megalocytiviral ORFs using RBIV-TY1 (Do et al., 2004) as reference, other numbers indicated megalocytiviral ORFs using ISKNV (He et al., 2001) as reference.

Viral infection can induce cells to express stress proteins. For instance, stress proteins have been associated with the polyomavirus, Simian virus 40, rabies virus, vesicular stomatitis virus, and the Sindbis virus (Cho et al., 1997). Although the mechanisms of stress protein induction and the subsequent roles of these proteins during viral infection remain unclear, the function of chaperone proteins that are expressed during viral infection has been hypothesized to facilitate the folding and/or assembly of viral proteins (Cho et al., 2002). Furthermore, viral infections in fish elicited antibodies against the virus-inducible stress protein (VISP), which could protect against subsequent infections of a fish rhabdovirus, infectious hematopoietic necrosis virus (IHNV) (Lee et al., 1996).

Aside from the viral proteins, cellular proteins are always involved in virion assembly and composition, and some of these proteins have been confirmed to participate in viral infection, pathogenicity, and immunity (Amet et al., 2012; Arita et al., 2012; Lee et al., 1996; Li et al., 2012; Shaw et al., 2008). In this study, a total of 33 cellular proteins were identified from purified SKIV by the 1-DE LC–MS/MS approach. The full genome of mandarin fish has not been sequenced, which restricts the identification of cellular proteins. Consequently, most of the identified cellular proteins are matched to those from other fish species (Table 3). Among these cellular proteins, mVISP was confirmed as one of the most abundant proteins in purified SKIV virions by both 1-DE-based MALDI-TOF-MS/MS (Fig. S1) and LC–MS/MS approaches (Table S2). As shown in Fig. 1B, mVISP was the structural protein with the fourth highest molecular mass in the purified SKIV virions, which was clearly visualized by staining with CBB-R250 (Fig. 1B). Then, mVISP was further confirmed to be the outermost protein surrounding the SKIV virions by the WB and IEM analyses. In megalocytiviruses, the outermost component that is located outside the MCP is defined as the viral envelope (Dong et al., 2011). In a previous proteomic analysis of ISKNV, this protein was identified as an unknown protein although it is the VISP homolog of purified ISKNV (Dong et al., 2011). In the present study, we provide the first report on the identification of mVISP as a novel cellular envelope protein in SKIV virions. Thus, including ISKNV-ORF007, -ORF056 and -ORF118, a total of four envelope proteins, including mVISP, have already been identified in megalocytiviruses. In addition, mVISP was the only cellular envelope protein that was highly abundance in the purified virions.

*Ot*VISP was first reported as an important virion-associated protein in purified IHNV (Lee et al., 1996). The protein was

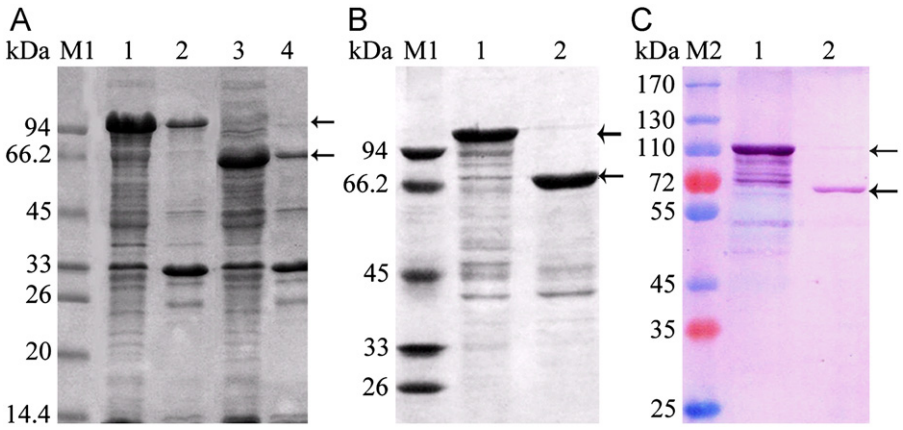

Fig. 3. Expression, purification, and antigenic analysis of the partial fractions of recombinant mVISP. (A) Prokaryotic expression of two fragments of mVISP using pMAL-cx2 expression vector. Lanes 1 and 3 indicate the soluble fractions of recombinant pMAL-cx2-F1 and pMAL-cx2-F2, respectively. Lanes 2 and 4 indicate the insoluble fractions of recombinant pMAL-cx2-F1 and pMAL-cx2-F2, respectively. (B) Purified recombinant pMAL-cx2-F1 and pMAL-cx2-F2 from the soluble recombinant complexes using the pMAL-cx2 purification system. (C) Antigenic analysis of two recombinant fractions of mVISP using rabbit anti-ISKNV serum as the primary antibody. Arrows indicate the corresponding recombinant fractions of pMAL-cx2-F1 and pMAL-cx2-F2.

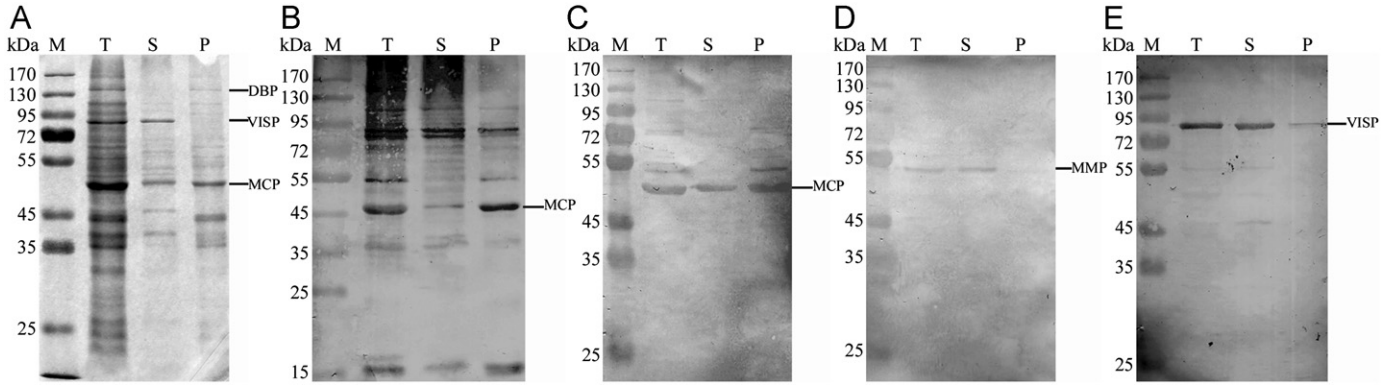

Fig. 4. Location of mVISP by WB. Supernatant and pellet fractions of the SKIV viral proteins were isolated by 1% Triton X-100, and (A) separated by 12% SDS-PAGE. The proteins were analyzed by WB using purified rabbit anti-sera against (B) ISKNV, (C) rMCP, (D) rMMP and (E) r-mVISP-F2. M, pre-stained broad range protein molecular mass marker. T, total purified protein of SKIV virions. S, supernatant fraction of detergent-treated SKIV virions. P, pellet fraction of detergent-treated SKIV virions.

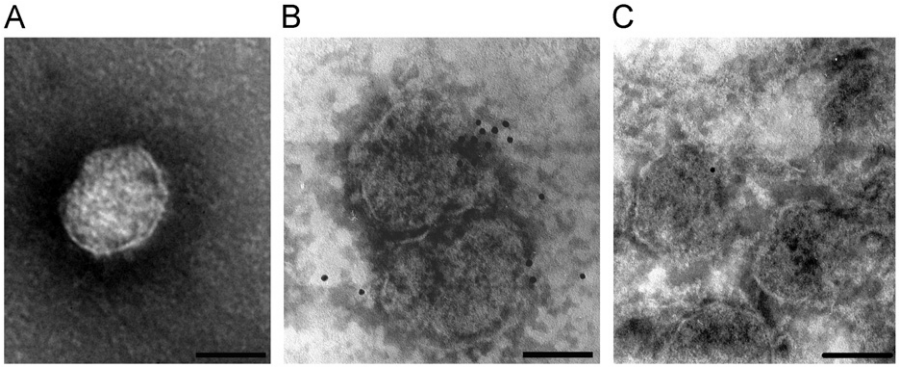

Fig. 5. Localization of mVISP in the SKIV virions by immunoelectron microscopy. The purified viral particles and Triton-X-100 treated virions were adsorbed onto Formvar-coated, carbon-stabilized, 200 mesh nickel grids. After incubation in the anti-serum against mVISP-F2 and the pre-immune serum, the goat anti-rabbit IgG conjugated 10 nm colloidal gold was used as the secondary antibody. The specimens were examined under a transmission electron microscope. (A) Triton-X-100 treated SKIV virion was detected using immunogold-labeled anti-mVISP antibodies; (B) Purified virus particles were detected using immunogold-labeled anti-mVISP antibodies. (C) Pre-immune rabbit serum was used as a negative control. Scale bar = 100 nm.

subsequently characterized as a novel 90 kDa chaperone-like protein that is distinct from the well-known 90 kDa chaperone protein of hsp90 (Cho et al., 1997, 2002). More importantly, the monoclonal antibody against *Ot*VISP was confirmed to have high neutralization activity *in vitro*. Thus, *Ot*VISP was presumed to be a promising candidate for the preparation of genetic vaccines against IHNV (Lee et al., 1996). In the present study, we demonstrated that mVISP was a highly abundant envelope protein in SKIV virions. The antibody against purified ISKNV could effectively recognize the recombinant mVISP fractions (Fig. 2C), which strongly suggested that mVISP was immunogenic. The time course of mVISP protein expression indicated that mVISP protein showed a similar expression pattern to that of MCP in the late stage of SKIV infection (Fig. 6). Viral envelope protein locates outermost layer in virion

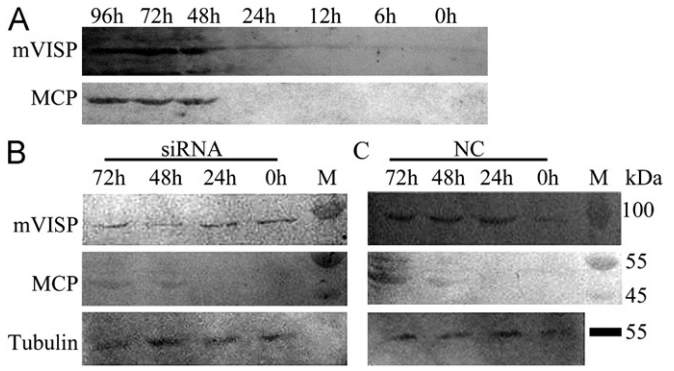

Fig. 6. Western blotting analysis of mVISP and MCP protein expression in normal (A), mVISP target siRNA knockdown (B) and non-silencing control (C) SKIV-infected MFF-1 cells, respectively.

and is always conceived to play important role in early viral infection and replication. In ranavirus, knockdown of FV3-ORF053R, a homologous envelope protein to ISKNV-ORF007, was evidenced to significantly affect the viral replication (Whitley et al., 2010). However, in this study, knockdown of mVISP showed no effect on virion production. The virus suspension from siRNA and NC groups showed similar viral titers. Furthermore, *in vitro* neutralization test showed that the two antibodies based on the recombinant mVISP fractions could not prevent SKIV infection in MFF-1 cells (data not shown). All these data indicated mVISP was not a crucial factor in SKIV viral infection and production.

Other well-studied virion-associated cellular proteins were likewise discovered by LC–MS/MS analysis, which included the glucose-regulated protein 78 (GRP78), voltage-dependent anion channel (VDAC), and the valosin-containing protein (VCP) family, among others. These cellular proteins from human or other mammals have been extensively studied and are known to function in intercellular antiviral and viral pathogenesis (Chen et al., 2011; Li et al., 2012; Ma et al., 2009). For example, GPR78 was demonstrated as an endogenous anti human Hepatitis B virus factor (Ma et al., 2009); VCP/p97 is involved in cellular protein secretion pathway in poliovirus infection involved in cellular protein secretion pathway in human poliovirus infection (Aritaet al., 2012); Most recently, VDAC 2 was confirmed to play a crucial role in chicken infectious bursal disease virus (IBDV)-induced apoptosis via interacting with IBDV-VP5 (Li et al., 2012). In addition, 14 translation-associated ribosomal proteins were also identified. Because ribosomal proteins were not found in other viral proteomics studies, it is still uncertain whether these proteins are true component packaged into SKIV virions or contaminating host proteins. However, ribosomal genes have been extensively explored in iridovirus-induced differential expression analysis in infected tissues or cells (He et al., 2006; Yeh et al., 2008). In He et al. (2006) and Yeh et al.'s (2008) studies, both ribosomal genes were found the most abundant differential genes and 17 and 13 ribosomal genes were found involving down-regulation expression in ISKNV infection mandarin fish spleen tissue and GIV infection GK-2 cell line, respectively (He et al., 2006; Yeh et al., 2008). Overall, 33 cellular proteins were identified from purified SKIV virions using reverse nano-LC MS/MS. Unlike the high abundance of mVISP, other cellular proteins were not abundant and not detected by 1-DE-based MALDI-TOF/TOF-MS. In aquatic virus field, studies on the mechanisms of host–virus interactions are still limited and elusive. Future studies should localize these cellular proteins in the structure of megalocytiviral virions, explore their interaction nets with viral proteins and other cellular proteins, as well as elucidate their roles in viral morphogenesis, pathogenesis, and immunity.

Materials and methods

Virus, cell lines, and antibodies

The SKIV-ZJ07 viral strain and the MFF-1 cell lines were characterized and maintained in our laboratory (Dong et al., 2008, 2010). The rabbit anti-ISKNV-NH060831, ISKNV-MCP and ISKNV-MMP (ISKNV-ORF-007 target protein) sera were prepared and stored in our laboratory as previously described (Dong et al., 2011).

SKIV propagation and purification

MFF-1 cells were cultured in Dulbecco's modified Eagle's medium (DMEM), which was supplemented with 10% fetal bovine serum (FBS) (Gibco, USA), 100 U/ml penicillin, 100 mg/ml streptomycin, and 0.25 g/ml amphotericin B (Invitrogen). When the MFF-1 cells became confluent, the cells were infected with SKIV at a multiplicity of infection (MOI) of 1. Four to five days post-infection, the infected MFF-1 cells were collected and subsequently stored at −80 °C. The frozen infected cells were freeze-thawed thrice to purify the SKIV virus. The cell debris was pelleted at 8000 rpm for 30 min at 4 °C, and the resultant cell-free supernatant was centrifuged at 30,000 rpm in a Beckman type 70 Ti rotor for 30 min at 4 °C. The virus pellet was resuspended in TNE buffer (50 mM Tris–HCl, 150 mM NaCl, 1 mM disodium EDTA, ethylenediaminetetraacetic acid; pH, 7.4; 4 °C) and carefully layered onto 30%, 40%, 50%, and 60% (w/v) sucrose gradients. After 2 h of centrifugation at 150,000 × *g* at 4 °C in a Beckman SW40 Ti rotor, the viral layer was located between the 50% and 60% sucrose layers. The viral band was then removed and resuspended in the TNE buffer. The virion pellets were finally collected after 30 min of centrifugation at 150,000 × *g* at 4 °C and suspended in TN buffer (50 mM Tris–HCl, 150 mM NaCl; pH 7.4; 4 °C). The viral purity was determined using TEM. The viral protein concentrations were then measured by the Bradford assay, prior to storage at −80 °C.

Viral protein identification by MS analysis

The purified SKIV virions were separated by 12% SDS-PAGE and visualized by staining with fresh Coomassie brilliant blue R250 (CBB-R250). The stained protein bands (Fig. 1C, lane 1) were excised separately from gels, cut into pieces, and transferred into a 1.5 ml microcentrifuge tube. The gel pieces were washed twice with 50% acetonitrile in 50 mM ammonium bicarbonate for 20 min per wash, dehydrated with 100% acetonitrile for 10 min, and vacuum dried. For enzymatic digestion, 125 ng of modified trypsin (sequencing grade; Promega) was dissolved in 10 μl of 50 mM ammonium bicarbonate and gradually added to the dry gel pieces. The samples were reswollen at 4 °C for 30 min and incubated overnight at 37 °C. Following digestion, the tryptic peptides were extracted twice with 60 μl of 50% acetonitrile and 0.1% trifluoroacetic acid for 30 min per extraction. The extracted solutions were pooled and vacuum dried for the subsequent MALDI-time-of-flight (TOF)-MS/MS analysis. The MALDI mass spectra were obtained using a 4700 Proteomics Analyzer with tandem TOF (TOF/TOF) optics (Applied Biosystems) fitted with a 355 nm Nd:YAG laser. These spectra were acquired using the positive-ion reflector mode with an acceleration voltage of 20 kV. The high intensity parent ions were selected and fragmented using collision-induced dissociation. The spectra were internally calibrated with peptides from trypsin autolysis. The proteins were identified by their peptide mass fingerprints (PMFs) and confirmed by the MS/MS analysis of two peptides in each sample. Instrumental control was achieved with the 4700 Explorer

software. Meanwhile, the GPS Explorer software was used to process data and to search non-redundant databases at the National Center for Biotechnology Information (NCBI) using the Mascot platform (Matrix Science, London, United Kingdom) with the following parameters: peptide mass fingerprint, 0.3 Da; MS/MS sequence tag, 0.4 Da; and allowing one un-cleaved tryptic site, as well as the oxidation of methionine and the carbamidomethylation of cysteines. The PMFs were used to query the NCBInr dsDNA virus protein database using the MASCOT program (http://www.matrixscience.com).

In-gel digestion and LC–MALDI MS/MS analysis

For the LC–MS/MS analysis, the gel lane with the separated viral proteins (Fig. 1C, lane 2) was cut into three pieces. Each gel piece was ground into fine particles, suspended with approximately 5 volumes of 0.1% SDS and 50 mM Tris–HCl (pH, 8.5), and incubated at 100 °C with intermittent vortex mixing until the viscous lump had disappeared. After centrifugation, the supernatant was retrieved and its protein concentration was determined using the RC DC protein assay kit (Bio-Rad). The extracted proteins were further diluted to 160 μl with 0.1% SDS, 50 mM Tris, pH, 8.5, and 4 μl of 50 mM tris (2-carboxyethyl) phosphine. The mixture was incubated at 100 °C for 10 min and allowed to cool. After a second incubation at 37 °C for 2 h in the dark, 40 μl of 50 mM iodoacetamide and Milli-Q water (200 μl) with 0.1 μg/μl sequencing-grade porcine trypsin were added to the sample, which was then incubated at 37 °C overnight. The digested peptides were subjected to LC–MALDI MS/MS analysis at the Research Center for Proteome Analysis (Shanghai, China), as described previously (Dong et al., 2011). The acquired MS/MS spectra were automatically used to search the GenBank virus protein database using the TurboSEQUEST program in the BioWorks 3.0 software package (version 3.1; Thermo). An acceptable SEQUEST result must have a delta correlation ($delC_n$) score of at least 0.1 (regardless of charge state) and a cutoff ranking during preliminary scoring (*Rsp*) of 4. The cross-correlation scores (X_{corr}) of matches were greater than 1.9, 2.2, and 3.75 for the charged states of 1, 2, and 3 peptide ions, respectively.

Cloning, expression, purification, and antigenic analysis of recombinant mVISP fractions

Total RNA was extracted from the SKIV-infected MFF-1 cells using the Trizol reagent (Invitrogen, USA). The total mRNA was reverse-transcribed into cDNA using the MMLV reverse transcriptase (Promega, USA) and random primers. The mVISP DNA fragment was amplified from the cDNA by polymerase chain reaction (PCR). The peptide information from mass spectrometry identification and the genetic sequence of the VISP from Chinook salmon (*Oncorhynchus tshawytscha*), designated as *Ot*VISP, which was taken from GenBank (GenBank Accession: AF527060.1), were used to design two forward primers (mVISP-F1: 5′-CGC*GGATCC*-CAATTATTAGATCCTG-3′ and mVISP-F2: 5′-CGC*GGATCC*AATGATA-AACACTATGC-3′ with the *Bam*HI restriction site) and one reverse primer (mVISP-R: 5′-CCC*AAGCTT*AAGTTCGAATTTATCACC-3′ with the *Hin*dIII restriction site) to amplify the corresponding mVISP fractions. The *Bam*HI and *Hin*dIII restriction sites were incorporated into the forward and reverse primers to facilitate their cloning into the pMAL-c2x expression vector (Merck, Germany). The PCR products were purified, digested, and cloned into the digested pMAL-c2x plasmid. The positive colonies were identified by restriction enzyme analysis and confirmed by DNA sequencing. The resultant plasmids were designated as pMAL-c2x-mVISP-F1 and pMAL-c2x-mVISP-F2 according to the forward primer that was used and transformed into the competent *Escherichia coli* BL21 (DE3) strain. Overnight cultures of the *E. coli* BL21 recombinant plasmids were diluted to 1:100 (vol/vol) in fresh Luria Broth with ampicillin (100 μg/ml) and incubated at 37 °C until the optical density at 600 nm was 0.6. A final concentration of 1 mM isopropyl-b-D-thiogalactopyranoside (IPTG) was added to the bacterial cultures, which were incubated for 4–6 h at 37 °C. The bacterial cells were harvested by centrifugation, washed, and resuspended in a buffer (0.1 M NaH_2PO_4, 10 mM Tris–HCl, pH, 8.0). The cell suspensions were disrupted by sonication on ice (at 300 W; thrice for 10 min each), and the cell lysates were centrifuged at 7000 × *g* for 15 min at 4 °C. The supernatants that contained the recombinant proteins were subsequently purified by affinity chromatography using the Amylose Resin (New England BioLabs) according to the manufacturer's instructions. The supernatants with the maltose-binding protein-β-galactosidase fusion protein (100,000 U) were passed through a 1 ml column at 4 °C. The column was then washed with 10 column volumes of a solution that contained 20 mM Tris–HCl (pH, 7.4), 0.2 M NaCl, 10 mM β-mercaptoethanol, and 1 mM EDTA. The mVISP proteins were eluted with a washing buffer that was supplemented with 10 mM maltose. The concentrations of the purified proteins were determined by the Bradford assay before they were stored at −80 °C. SDS-PAGE (12%) was performed to identify the individual purified proteins. Using the rabbit anti-ISKNV serum as the primary antibody, Western blot (WB) analysis was performed to assess the antigenicity of the purified recombinant mVISP proteins.

Preparation of anti-sera

New Zealand white rabbits that were maintained at the Laboratory Animal Research Center of Sun Yat-sen University, China were used to prepare the recombinant mVISP protein anti-sera. Two hundred and fifty microgram of each purified protein was mixed with an equal volume of complete Freund's adjuvant (Sigma, USA), and the mixture was subcutaneously injected into the rabbits. Booster immunizations of 250 μg purified protein mixed with an equal volume of Freund's incomplete adjuvant (Sigma, USA) were scheduled for each rabbit on days 15, 22, and 30 after the first immunization. Ten days after the last injection, the rabbits were sacrificed and their anti-sera were collected. The obtained anti-sera were stored at −80 °C until further use.

Location of mVISP in SKIV by WB analysis

The viral protein fraction was prepared based on a previously described procedure with minor modifications (Dong et al., 2011). In brief, the purified virus suspension was centrifuged at 20,000 × *g* for 15 min at 4 °C. The viral pellets were resuspended in a salt-containing TMN buffer (20 mM Tris–HCl, 150 mM NaCl, 2 mM $MgCl_2$; pH, 7.5). Triton X-100 was added with a final concentration of 1% to the viral suspension and incubated at room temperature (RT) for 3 min. Subsequently, the supernatant and pellet fractions of the samples were separated by centrifugation at 20,000 × *g* for 20 min at 4 °C. The pellet was rinsed with distilled water to eliminate any residual supernatant solution and resuspended in the TMN buffer. Finally, samples of the pellet or the supernatant were mixed with an equal volume of 2 × Laemmli sample buffer (62.5 mM Tris–HCl, pH, 6.8; 25% glycerol; 2% SDS; 0.01% Bromophenol Blue; 5%, v/v, β-mercaptoethanol).

The total viral protein, supernatant, and pellet fractions of the Triton X-100-treated viral proteins were separated by 12% SDS-PAGE. These proteins were then transferred onto nitrocellulose (NC) membranes (Whatman, UK) using a constant current of 200 mA for 2 h. The NC membranes were blocked with 5% fat-free milk in Tris-buffered saline (TBS; 0.02 M Tris–HCl, 0.5 M NaCl; pH,

7.5) at RT for 1 h. After being washed with TBS-T (0.05% Tween-20 in TBS) thrice for 10 min, the NC membranes were incubated with rabbit anti-mVISP-F2 serum (1:2000 dilution in TBS-T containing 1% BSA) at RT for 1 h. The membranes were washed thrice with TBS-T (each wash for 10 min), followed by incubation with the goat anti-rabbit IgG-conjugated alkaline phosphatase (Sigma, USA) secondary antibody (1:10,000 dilution). The membrane was then washed three more times with PBST (phosphate-buffered saline, PBS, with 0.2% Triton X-100) and visualized with fresh nitro blue tetrazolium (NBT)/5-bromo-4-chloro-3-indolyl-phosphate (BCIP) substrate solution. The rabbit anti-sera against ISKNV-MCP (the MCP homolog in SKIV) and ISKNV-VP007 (a myristylated membrane protein, MMP) were used as the first antibodies for similar WB analysis as control monitors.

Immunogold electron microscopy (IEM)

The purified SKIV viral particles and TX-100 treated viruses were adsorbed onto Formvar-coated, carbon-stabilized, 200 mesh nickel grids. After semi-drying for 15 min, the grids were blocked with 2% BSA for 30 min at 37 °C. The grids were rinsed with PBS and incubated with rabbit anti-mVISP-F2 (1:100 dilution) for 1 h at 37 °C. The pre-immune serum from rabbit was used as the negative control. After washing with PBS, the grids were incubated with goat anti-rabbit IgG conjugated to 10 nm colloidal gold (Sigma, USA) for 60 min at 37 °C. The grids were then washed with PBS and negatively stained with 2% phosphotungstic acid (PTA). The specimens were examined under a transmission electron microscope (JEM-100CX II, Japan).

Time course expression of mVISP in SKIV-infected MFF-1 cells by WB analysis

MFF-1 cells were grown in 25 cm^2 tissue culture flasks until 90% confluence was observed, and these were subsequently infected with the SKIV-ZJ07 suspension (MOI=1). After incubation for 1 h at 27 °C, the growth medium was replaced with the maintenance medium (DMEM plus 2.5% FBS). The infected cells at 0, 6, 12, 24, 48, 72, and 96 h post-infection (hpi) were digested by trypsinization and collected by centrifugation at 800 × *g* for 3 min at room temperature. After rinsing with sterile PBS once for 3 min at room temperature, the total cellular proteins were extracted using lysis buffer. The protein concentration was determined by Bradford method according to operation manual. The total proteins were separated by 12% SDS-PAGE and followed by Western blotting analysis. The rabbit anti-sera of mVISP-F2 and ISKNV-MCP were used as the first antibodies.

Knockdown of mVISP expression by siRNA method

The sequence sets for mVISP-specific siRNA (5′–GCAAUU-GACCGUGAAGAAUTT-3′ and 5′-AUUCUUCACGGUCAAUUGCTT-3′) and a non-silencing control siRNA (5′-UUCUCCGAACGUGUCAC-GUTT-3′ and 5′-ACGUGACACGUUCGGAGAATT-3′) were used for mVISP knockdown. The siRNA specific for mVISP was designed using the BLOCK-iT™ RNAi Designer on the Invitrogen website and synthesized by the Invitrogen Company. To transfect the mVISP target siRNA, 100 pmol of siRNA and 5 μl of lipofectamine 2000 (Invitrogen) were separately diluted in 250 μl of serum free Opti-MEM medium and incubated at room temperature for 5 min. The two solutions were mixed and incubated at room temperature for 15 min, after which the mixture was added to MFF-1 cells that had been pre-seeded in 35-mm Petri dishes. MFF-1 cells were transfected 100 pM non-silencing control siRNA (siRNA-negative) as a negative control. After 4–6 h incubation, the siRNA-transfected MFF-1 cells were replaced with DMEM medium plus 10% FBS and infected with SKIV-ZJ07. The SKIV-infected cells were harvested at 0, 24, 48, 72 hpi and washed with PBS. Partial yielded virus suspensions were used to determine $TCID_{50}$ in normal MFF-1 cells. Other SKIV-infected cells were collected. Total proteins were extracted using 100 μl lysis buffer for Western blot analysis. The anti-sera against mVISP-F2, ISKNV-MCP and Beta-Tubulin (Invitrogen) were used as the first antibodies.

Acknowledgments

This research was supported by the special supporting project 201003385 of the China Postdoctoral Science Foundation; the National Basic Research Program of China under Grant no. 2012CB114406; the Technology Planning Project of Guangdong Province under Number 2011A020102002 and the Planning subject of 'the Twelfth Five-Year-Plan' in National Science and Technology for the Rural Development in China under Number 2011BAD13B00.

Appendix A. Supporting information

Supplementary data associated with this article can be found in the online version at http://dx.doi.org/10.1016/j.virol.2012.12.017.

References

Amet, T., Ghabril, M., Chalasani, N., Byrd, D., Hu, N., Grantham, A., Liu, Z., Qin, X., He, J.J., Yu, Q., 2012. CD59 incorporation protects hepatitis C virus against complement-mediated destruction. Hepatology 55 (2), 354–363.

Arita, M., Wakita, T., Shimizu, H., 2012. Valosin-containing protein (VCP/p97) is required for poliovirus replication and is involved in cellular protein secretion pathway in poliovirus infection. J. Virol. 86 (10), 5541–5553.

Chen, I.T., Aoki, T., Huang, Y.T., Hirono, I., Chen, T.C., Huang, J.Y., Chang, G.D., Lo, C.F., Wang, H.C., 2011. White spot syndrome virus induces metabolic changes resembling the warburg effect in shrimp hemocytes in the early stage of infection. J. Virol. 85 (24), 12919–12928.

Chinchar, V.G., Essbayer, S., He, J.G., Hyatt, A., Miyazaki, T., Seligy, V., Williams, T., 2005. Family Iridoviridae. In: Fauquet, C.M., Mayo, M.A., Maniloff, J., Desselberger, U., Ball, L.A. (Eds.), Virus Taxonomy: 8th Report of the International Committee on the Taxonomy of Viruses. Elsevier Academic Press, San Diego, CA, USA, pp. 163–175.

Cho, W.J., Cha, S.J., Do, J.W., Choi, J.Y., Lee, J.Y., Jeong, C.S., Cho, K.J., Choi, W.S., Kang, H.S., Kim, H.D., Park, J.W., 1997. A novel 90-kDa stress protein induced in fish cells by fish rhabdovirus infection. Biochem. Biophys. Res. Commun. 233 (2), 316–319.

Cho, W.J., Yoon, W.J., Moon, C.H., Cha, S.J., Song, H., Cho, H.R., Jang, S.J., Chung, D.K., Jeong, C.S., Park, J.W., 2002. Molecular cloning of a novel chaperone-like protein induced by rhabdovirus infection with sequence similarity to the bacterial extracellular solute-binding protein family 5. J. Biol. Chem. 277 (44), 41489–41496.

Do, J.W., Moon, C.H., Kim, H.J., Ko, M.S., Kim, S.B., Son, J.H., Kim, J.S., An, E.J., Kim, M.K., Lee, S.K., Han, M.S., Cha, S.J., Park, M.S., Park, M.A., Kim, Y.C., Kim, J.W., Park, J.W., 2004. Complete genomic DNA sequence of rock bream iridovirus. Virology 325 (2), 351–363.

Dong, C., Weng, S., Luo, Y., Huang, M., Ai, H., Yin, Z., He, J., 2010. A new marine megalocytivirus from spotted knifejaw, *Oplegnathus punctatus*, and its pathogenicity to freshwater mandarinfish, *Siniperca chuatsi*. Virus Res. 147 (1), 98–106.

Dong, C., Weng, S., Shi, X., Xu, X., Shi, N., He, J., 2008. Development of a mandarin fish Siniperca chuatsi fry cell line suitable for the study of infectious spleen and kidney necrosis virus (ISKNV). Virus Res. 135 (2), 273–281.

Dong, C., Xiong, X., Luo, Y., Weng, S., Wang, Q., He, J., 2012. Efficacy of a formalin-killed cell vaccine against infectious spleen and kidney necrosis virus (ISKNV) and immunoproteomic analysis of its major immunogenic proteins. Vet. Microbiol., http://dx.doi.org/10.1016/j.vetmic.2012.10.026.

Dong, C.F., Xiong, X.P., Shuang, F., Weng, S.P., Zhang, J., Zhang, Y., Luo, Y.W., He, J.G., 2011. Global landscape of structural proteins of infectious spleen and kidney necrosis virus. J. Virol. 85 (6), 2869–2877.

Fu, X., Li, N., Liu, L., Lin, Q., Wang, F., Lai, Y., Jiang, H., Pan, H., Shi, C., Wu, S., 2011. Genotype and host range analysis of infectious spleen and kidney necrosis virus (ISKNV). Virus Genes 42 (1), 97–109.

Go, J., Lancaster, M., Deece, K., Dhungyel, O., Whittington, R., 2006. The molecular epidemiology of iridovirus in Murray cod (*Maccullochella peelii peelii*) and dwarf gourami (*Colisa lalia*) from distant biogeographical regions suggests a

link between trade in ornamental fish and emerging iridoviral diseases. Mol. Cell. Probes 20 (3–4), 212–222.
He, J.G., Deng, M., Weng, S.P., Li, Z., Zhou, S.Y., Long, Q.X., Wang, X.Z., Chan, S.M., 2001. Complete genome analysis of the mandarin fish infectious spleen and kidney necrosis iridovirus. Virology 291 (1), 126–139.
He, J.G., Zeng, K., Weng, S.P., Chan, S.M., 2000. Systemic disease caused by an iridovirus-like agent in cultured mandarinfish, *Siniperca chuatsi* (Basillewsky), in China. J. Fish Dis. 23, 219–222.
He, J.G., Zeng, K., Weng, S.P., Chan, S.M., 2002. Experimental transmission, pathogenicity and physical-chemical properties of infectious spleen and kidney necrosis virus (ISKNV). Aquaculture 204 (1–2), 11–24.
He, W., Yinlt, Z.X., Li, Y., Huo, W.L., Guan, H.J., Weng, S.P., Chan, S.M., He, J.G., 2006. Differential gene expression profile in spleen of mandarin fish *Siniperca chuatsi* infected with ISKNV, derived from suppression subtractive hybridization. Dis. Aquat. Org. 73 (2), 113–122.
Ince, I.A., Boeren, S.A., van Oers, M.M., Vervoort, J.J., Vlak, J.M., 2010. Proteomic analysis of Chilo iridescent virus. Virology 405 (1), 253–258.
Inouye, K., Yamano, K., Maeno, Y., Nakajima, K., Matsuoka, M., Wada, Y., Sorimachi, M., 1992. Iridovirus infection of cultured red sea bream. *Pagrus major*. Fish Pathol. 27, 19–27.
Jancovich, J.K., Chinchar, V.G., Hyatt, A., Miyazaki, T., Williams, T., Zhang, Q.Y., 2012. Family Iridoviridae. In: King, A.M.Q., Adams, M.J., Carstens, E.B., Lefkowitz., E.J. (Eds.), Virus Taxonomy: Ninth Report of the International Committee on Taxonomy of Viruses.. Elsevier Academic Press, San Diego, CA, pp. 193–210.
Kawakami, H., Nakajima, K., 2002. Cultured finfish species affected by red sea bream iridoviral disease from 1996 to 2000. Fish Pathol. 37 (1), 45–47.
Kurita, J., Nakajima, K., 2012. Review: Megalocytiviruses. Viruses 4, 521–538.
Kwon, S.R., Nishizawa, T., Park, J.W., Oh, M.J., 2011. Shift of phylogenic position in megalocytiviruses based on three different genes. J. Microbiol. 49 (6), 981–986.
Lee, J.Y., Cho, W.J., Do, J.W., Kim, H.J., Park, J.W., Park, M.A., Sohn, S.G., Jeong, G., Hah, Y.C., 1996. Monoclonal antibodies raised against infectious haematopoietic necrosis virus (IHNV) G protein and a cellular 90 kDa protein neutralize IHNV infection in vitro. J. Gen. Virol. 77 (Pt 8), 1731–1737.
Li, Z., Wang, Y., Xue, Y., Li, X., Cao, H., Zheng, S.J., 2012. Critical role for voltage-dependent anion channel 2 in infectious bursal disease virus-induced apoptosis in host cells via interaction with VP5. J. Virol. 86 (3), 1328–1338.
Lü, L., Zhou, S.Y., Chen, C., Weng, S.P., Chan, S.M., He, J.G., 2005. Complete genome sequence analysis of an iridovirus isolated from the orange-spotted grouper, *Epinephelus coioides*. Virology 339 (1), 81–100.
Ma, H., Xie, J., Weng, S., Zhou, T., He, J., 2012. Co-infection of megalocytivirus and viral nervous necrosis virus in a very severe mass mortality of juvenile orange-spotted groupers (*Epinephelus coioides*). Aquaculture 358–359, 170–175.
Ma, Y., Yu, J., Chan, H.L., Chen, Y.C., Wang, H., Chen, Y., Chan, C.Y., Go, M.Y., Tsai, S.N., Ngai, S.M., To, K.F., Tong, J.H., He, Q.Y., Sung, J.J., Kung, H.F., Cheng, C.H., He, M.L., 2009. Glucose-regulated protein 78 is an intracellular antiviral factor against hepatitis B virus. Mol. Cell. Proteomics 8 (11), 2582–2594.
Marcos-López, M., Feist, S.W., Hicks, R., Noguera, P.A., 2011. Systemic megalocytivirus infection in three-spined stickleback *Gasterosteus aculeatus*. Bull. Eur. Assoc. Fish Pathol. 31 (6), 227–234.
Nakajima, K., Maeno, Y., Yokoyama, K., Kaji, C., Manabe, S., 1998. Antigen analysis of red sea bream iridovirus and comparison with other fish iridoviruses. Fish Pathol. 33, 73–78.
Shaw, M.L., Stone, K.L., Colangelo, C.M., Gulcicek, E.E., Palese, P., 2008. Cellular proteins in influenza virus particles. PLoS Pathog. 4 (6), e1000085.
Shi, C.Y., Jia, K.T., Yang, B., Huang, J., 2010. Complete genome sequence of a Megalocytivirus (family Iridoviridae) associated with turbot mortality in China. Virol. J. 7, 159.
Song, W., Lin, Q., Joshi, S.B., Lim, T.K., Hew, C.L., 2006. Proteomic studies of the Singapore grouper iridovirus. Mol. Cell. Proteomics 5 (2), 256–264.
Song, W.J., Qin, Q.W., Qiu, J., Huang, C.H., Wang, F., Hew, C.L., 2004. Functional genomics analysis of Singapore grouper iridovirus: complete sequence determination and proteomic analysis. J. Virol. 78 (22), 12576–12590.
Subramaniam, K., Shariff, M., Omar, A.R., Hair-Bejo, M., 2012. Megalocytivirus infection in fish. Rev. Aquaculture 4, 221–233.
Waltzek, T.B., Marty, G.D., Alfaro, M.E., Bennett, W.R., Garver, K.A., Haulena, M., Weber 3rd, E.S., Hedrick, R.P., 2012. Systemic iridovirus from threespine stickleback *Gasterosteus aculeatus* represents a new megalocytivirus species (family Iridoviridae). Dis. Aquat. Org. 98 (1), 41–56.
Wang, Y.Q., Lu, L., Weng, S.P., Huang, J.N., Chan, S.M., He, J.G., 2007. Molecular epidemiology and phylogenetic analysis of a marine fish infectious spleen and kidney necrosis virus-like (ISKNV-like) virus. Arch. Virol. 152 (4), 763–773.
Wang, Z.L., Xu, X.P., He, B.L., Weng, S.P., Xiao, J., Wang, L., Lin, T., Liu, X., Wang, Q., Yu, X.Q., He, J.G., 2008. Infectious spleen and kidney necrosis virus ORF48R functions as a new viral vascular endothelial growth factor. J. Virol. 82 (9), 4371–4383.
Whitley, D.S., Yu, K., Sample, R.C., Sinning, A., Henegar, J., Norcross, E., Chinchar, V.G., 2010. Frog virus 3 ORF 53R, a putative myristoylated membrane protein, is essential for virus replication in vitro. Virology 405 (2), 448–456.
Xu, X., Huang, L., Weng, S., Wang, J., Lin, T., Tang, J., Li, Z., Lu, Q., Xia, Q., Yu, X., He, J., 2010a. Tetraodon nigroviridis as a nonlethal model of infectious spleen and kidney necrosis virus (ISKNV) infection. Virology 406 (2), 167–175.
Xu, X., Weng, S., Lin, T., Tang, J., Huang, L., Wang, J., Yu, X., Lu, L., Huang, Z., He, J., 2010b. VP23R of infectious spleen and kidney necrosis virus mediates formation of virus-mock basement membrane to provide attaching sites for lymphatic endothelial cells. J. Virol. 84 (22), 11866–11875.
Xu, X., Lin, T., Huang, L., Weng, S., Wei, W., Li, Z., Lu, L., Huang, Z., He, J., 2011. VP15R from infectious spleen and kidney necrosis virus is a non-muscle myosin-II-binding protein. Arch. Virol. 156 (1), 53–61.
Xu, X., Zhang, L., Weng, S., Huang, Z., Lu, J., Lan, D., Zhong, X., Yu, X., Xu, A., He, J., 2008. A zebrafish (*Danio rerio*) model of infectious spleen and kidney necrosis virus (ISKNV) infection. Virology 376 (1), 1–12.
Yeh, C.H., Chen, Y.S., Wu, M.S., Chen, C.W., Yuan, C.H., Pan, K.W., Chang, Y.N., Chuang, N.N., Chang, C.Y., 2008. Differential display of grouper iridovirus-infected grouper cells by immunostaining. Biochem. Biophys. Res. Commun. 372 (4), 674–680.